(15) W. Hässelbarth and E. Ruch, *Theor. Chim. Acta*, **29**, 259 (1973).
(16) W. G. Klemperer, *J. Chem. Phys.*, **56**, 5478 (1972); *J. Am. Chem. Soc.*, **94**, 6940 (1972); **95**, 380 (1973).
(17) J. Brocas and R. Willem, *Bull. Soc. Chim. Belg.*, **82**, 469 (1973).
(18) This is equivalent to the use of permutation–inversion operations by Longuet-Higgins.[19] Use of this operation was also necessary in triarylmethanes, which are also skeletally chiral.[2h,k,p]
(19) H. C. Longuet-Higgins, *Mol. Phys.*, **6**, 445 (1963).
(20) If instead one uses the pure permutation group ($\mathbf{R}_{128}$), the number of isomers has to be doubled in order to account for helicity. Use of the permutation–inversion group accomplishes this doubling, since, in this case, the permutation–inversion group ($\mathbf{G}_{256}$) is a direct product of the permutation group ($\mathbf{R}_{128}$) with $\mathbf{C}_{i^*}$. Thus, the size of **G** is doubled, but the conjugacy classes containing the elements in $\mathbf{R}_{128}$ remain the same.
(21) To calculate the number of isomers for a racemic or meso configuration of an *ab*CHCH*ab* skeleton separately, one uses for **G** the group $\mathbf{G}_{128} = (\mathbf{S}_2 \times \mathbf{S}_2)\ [\mathbf{S}_2] \times \mathbf{C}_{i^*} = \mathbf{R}_{64} \times \mathbf{C}_{i^*}$, which includes rigid rotations and inversion of *both* centers, but not inversion of a single center.[11]
(22) J. G. Nourse, *Proc. Natl. Acad. Sci. U.S.A.*, **72**, 2385 (1975).
(23) M. J. S. Dewar, S. Kirschner, H. W. Kollmar, and L. E. Wade, *J. Am. Chem. Soc.*, **96**, 5242 (1974).
(24) M. H. Chisholm and M. Extine, *J. Am. Chem. Soc.*, **97**, 5625 (1975).
(25) A. Hoekstra and A. Vos, *Acta Crystallogr., Sect. B*, **31**, 1716, 1722 (1975).
(26) J. F. Blount, personal communication.
(27) N. C. Baenziger, R. E. Buckles, and T. D. Simpson, *J. Am. Chem. Soc.*, **69**, 3405 (1967).
(28) H. E. Zimmerman and D. H. Paskovich, *J. Am. Chem. Soc.*, **86**, 2149 (1964).
(29) J. A. Valenzuela and A. J. Bard, *J. Phys. Chem.*, **72**, 286 (1968).
(30) This assignment is also consistent with the observation that meso 1,1,2,2-tetraarylethane derivatives generally have higher melting points than the corresponding racemic forms.[6]
(31) A decision between $\mathbf{C}_2$ and $\mathbf{C}_i$ skeletal symmetry could in principle be made by examining the NMR spectra in the presence of a chiral auxiliary reagent (solvent or shift reagent), since resonance doubling is possible for the diastereomeric mixture AA/BB ($\mathbf{C}_2$) but not for the diastereomeric mixture G/H ($\mathbf{C}_i$).
(32) Elemental analyses were performed by Professor G. Lo Vecchio at the University of Messina, Messina, Italy. Unless specified otherwise, NMR spectra were recorded on a Varian A-60D spectrometer at ambient temperature (ca. 40°) and refer to ca. 20% solutions in $CDCl_3$ containing tetramethylsilane (Me_4Si) as internal reference. Mass spectra were obtained on an AEI MS-9 high-resolution mass spectrometer, with an ionizing voltage of 70 eV. All reactions which involved the use of organometallic compounds as reagents were carried out under a dry high-purity nitrogen atmosphere. Melting points were measured in a Thomas-Hoover Apparatus and are corrected.

Stereochemical Analysis of 1,1,2,2-Tetraarylethanes. 2. Dynamic Stereochemistry of Selected Tetraarylethanes and the Use of Residual Stereoisomerism and Residual Stereotopism as a Tool for Differentiating among Divers Stereoisomerization Pathways

Paolo Finocchiaro,[1a] W. Douglas Hounshell,[1b] and Kurt Mislow*[1b]

Contribution from the Institute of Industrial Chemistry, University of Catania, 95125 Catania, Italy, and the Department of Chemistry, Princeton University, Princeton, New Jersey 08540. *Received November 24, 1975*

Abstract: The dynamic stereochemistry of 1,1,2,2-tetraarylethanes is treated using a group theoretical approach. The possible rearrangement modes for such systems are given and the ring-flip mechanisms associated with these modes are discussed. The temperature-dependent ^1H NMR spectra of 1,1,2,2-tetramesitylethane (TME) and of racemic and meso 1,2-dimesityl-1,2-bis(2,4,6-trimethoxyphenyl)ethane (**1**) indicate that a variety of stereochemical exchange phenomena take place on the NMR time scale. The lowest energy pathway for stereoisomerization in these molecules is found to be the four-ring flip. Because of the occurrence of correlated rotation of the aryl rings, residual diastereotopism is observed in such compounds under the four-ring flip. At higher temperatures, the residual signals of **1** undergo coalescence by an exchange process, which corresponds either to a three- or a two-ring flip. A method has been designed based on group theoretical considerations, which permits discrimination among various possible rearrangement modes by a study of the residual stereoisomerism and/or residual diastereotopism exhibited by appropriately substituted derivatives of 1,1,2,2-tetraphenylethane.

In the preceding paper[2] (hereafter referred to as part 1) we investigated the static stereochemistry of 1,1,2,2-tetraarylethanes (hereafter simply referred to as tetraarylethanes). On the basis of empirical force field calculations and ^1H NMR spectroscopic measurements, we concluded that these systems adopt a ground-state propeller conformation, with anti methine hydrogens and TPE (tetraphenylethane) skeletal $\mathbf{C}_2$ symmetry, provided the two edges of each aryl ring do not differ appreciably in steric requirement. The racemic and meso forms of 1,2-dimesityl-1,2-bis(2,4,6-trimethoxyphenyl)ethane (**1**) were separated and the configurations of the two isomers were established on the basis of their ^1H NMR spectra. It was also observed that tetramesitylethane (TME) and **1** exhibit restricted rotation of the aryl rings on the NMR time scale. Consequently, variable-temperature NMR studies are of interest as a means of providing information on the sites exchanged by the stereoisomerization processes which such systems are capable of undergoing, and on the energy requirements for these processes.

The present paper deals with the dynamic stereochemistry of TME and of **1**. We show how the use of a group theoretical approach is capable of providing the basis for a description of the possible rearrangement modes[3] in these systems, and for a facile interpretation of the great variety of stereochemical phenomena which can arise in more complex tetraarylethanes. In addition we demonstrate how this approach leads to a method involving the study of appropriately substituted derivatives of TPE, which can, in principle, be used to discriminate among the various possible rearrangement modes.

Rearrangement Modes and Flip Mechanisms

In the investigation of the static and dynamic stereochemistry of tri- and tetraarylmethane derivatives, we found it convenient to analyze chemical isomers and isomerizations by

Table I. Rearrangement Modes for Anti C_2 Tetraarylethanes[a-c]

M_1	M_2	M_3	M_4
(1)(2)(3)(4)(5)(6)(7)(8)	(34)	(12)	(12)(34)
(15)(26)(37)(48)	(15)(26)(3847)	(1625)(37)(48)	(1625)(3847)
	(78)	(56)	(56)(78)
	(15)(26)(3748)	(1526)(37)(48)	(1526)(3748)
M_5	M_6	M_7	M_8
(34)(56)	(34)(78)	(12)(56)	(12)(34)(56)
(1526)(3847)	(15)(26)(38)(47)	(16)(25)(37)(48)	(16)(25)(3847)
(12)(78)			(12)(56)(78)
(1625)(3748)			(16)(25)(3748)
M_9	M_{10}	M_{11}	M_{12a}
(12)(34)(78)	(12)(34)(56)(78)	(13)(24)(57)(68)*	(1324)(57)(68)*
(1625)(38)(47)	(16)(25)(38)(47)	(17)(28)(35)(46)*	(17)(28)(3645)*
(34)(56)(78)			(13)(24)(5768)*
(1526)(38)(47)			(1728)(35)(46)*
M_{12b}	M_{13}	M_{14}	M_{15a}
(1423)(57)(68)*	(14)(23)(57)(68)*	(1324)(5867)*	(1324)(5768)*
(1827)(35)(46)*	(1827)(3645)*	(17)(28)(36)(45)*	(1728)(3645)*
(13)(24)(5867)*	(13)(24)(58)(67)*	(1423)(5768)*	
(17)(28)(3546)*	(1728)(3546)*	(18)(27)(35)(46)*	
M_{15b}	M_{16a}	M_{16b}	M_{17}
(1423)(5867)*	(14)(23)(5867)*	(14)(23)(5768)*	(14)(23)(58)(67)*
(1827)(3546)*	(1827)(36)(45)*	(18)(27)(3645)*	(18)(27)(36)(45)*
	(1423)(58)(67)*	(1324)(58)(67)*	
	(18)(27)(3546)*	(1728)(36)(45)*	

[a] The permutational notation (site labeling) is described in part I. [b] Double cosets were calculated manually by Dr. Devens Gust, and independently by use of a computer program written in these laboratories by Mr. Gilbert Chin. [c] Modes with the same number but designated a or b are inverse double cosets.

applying simple group theoretical concepts.[4-6] In part 1 we used this approach to compute[7] the number of stereoisomers for any given substitution pattern in derivatives of TPE. In this section our analysis will be extended to the dynamic stereochemistry of tetraarylethanes in order to provide the background necessary for a discussion of our DNMR results.

There are, in principle, three general classes of stereoisomerizations which could be considered for a tetraarylethane. One of these classes involves rotation about the central C-C bond and thus interconverts anti and gauche rotamers. Another consists of processes in which inversion occurs at one or two chiral centers without affecting helicity[8] or ring motion. The third involves rotation of the aryl rings about their bonds to the central carbon atoms. These classes of isomerization processes (individually or in combination) can be subdivided into rearrangement modes[3] (racemic modes[7]). Molecular mechanics calculations have ruled out all but anti C_2 ground-state structures.[2] We can therefore disregard all mechanisms which lead to a structure with a different TPE skeletal symmetry, i.e, anti C_2 skeletal symmetry must be preserved in the initial and final states. It should also be noted that whether gauche or eclipsed rotamers are populated in the transition state of an isomerization mechanism is of no consequence, for permutational isomerizations (as well as NMR site exchanges) deal only with the net change from initial to final state and are not concerned with details of structure and energy along the reaction coordinate of the transformation.[5a,6,9,10]

In part 1, isomerizations were represented as permutations of ligands on numbered sites (edges). The group of order 24 necessary to describe all possible permutations of four aryl groups on an anti tetraarylethane skeleton (central rotation, and hence gauche rotamers, need not to be considered) was reduced to the ring permutation group $S_2[S_2]$ (where the first S_2 corresponds to the C_2 rotation and the second to inversion at one center) by considering only *stereo*isomerizations. The full permutation group ($\mathbf{R}_{128}$) was derived by combining the ring permutation group with the ring-flip group $(S_2)^4$; thus, $\mathbf{R}_{128} = (S_2[S_2])[S_2]$. Including helicity, the full permutation-inversion group of stereoisomerizations was found to be $\mathbf{G}_{256} = \mathbf{R}_{128} \times \mathbf{C}_{i*}$. If one further disallows inversion as a feasible operation under the conditions of the experiment (and thus includes only rotation of the aryl rings), he obtains the ring permutation group $S_2[S_1] \simeq C_2$, and thus the feasible permutation group $\mathbf{R}_{32} = (S_2[S_1])[S_2]$. Including reversal of helicity (h, as defined in part 1) results in the feasible permutation-inversion group[11] for tetraarylethanes, $\mathbf{R}_{32} \cup h\mathbf{R}_{32} = \mathbf{G}_{64}$.

The possible rearrangement modes for tetraarylethanes, considering only rotation of the aryl rings, correspond to the double cosets[7] of the point group (C_2) in the feasible permutation-inversion group ($\mathbf{G}_{64}$). The 20 double cosets[12] are listed in Table I. If one assumes microscopic reversibility, non-self-inverse double cosets are paired[5b] to reduce these 20 double cosets to 17 modes[13,14] (designated by the symbols $\mathbf{M}_j$, j = 1-17).

We will now confine further discussion to those seven modes ($\mathbf{M}_{11}$-$\mathbf{M}_{17}$) which involve a change in helicity (i.e., which constitute the elements in the $h\mathbf{R}_{32}$ coset), since the evidence shows that all *single-step* isomerizations of the analogous Ar_3Z[15] and Ar_3ZX[16] systems involve a change in helicity. These seven modes are the permutational consequences of seven classes of "flip" mechanisms,[8,16a,17] i.e., the zero-, one-, three different two-, three-, and four-ring flips (see Figure 1). In these mechanisms, zero, one, two, three, or all four aryl rings, respectively, "flip", i.e., rotate about their C_{aryl}-C_{ethane} bond and pass through a 0° dihedral angle (defined in part 1), while the remaining rings rotate in the opposite direction and pass through a 90° dihedral angle ("nonflip"). The product and starting molecules thus have opposite helicities.

Since there are four aryl groups in the molecule and each aryl ring has two differentiable edges, the ring flip permutation group is $(S_2)^4$. There are thus a total of 16 flip mechanisms

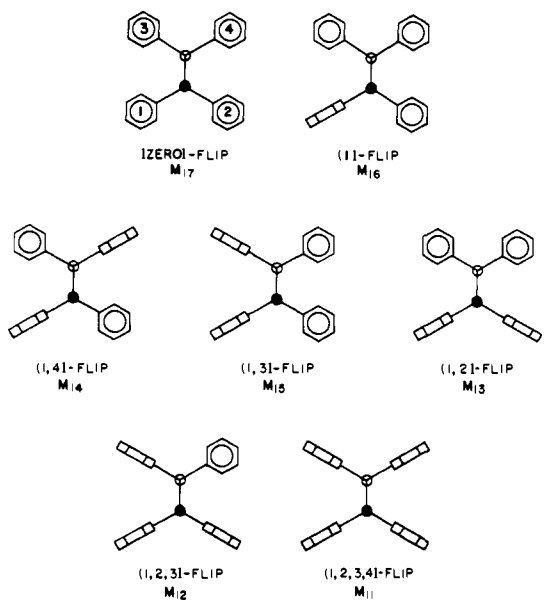

Figure 1. Idealized transition states of the rotational (flip) mechanisms associated with each rearrangement mode for tetraphenylethane in the anti conformation.

whose net effect can be represented by the following 16 permutations: one in which zero rings flip ($\mathbf{M}_{17}$); four in which one ring flips ($\mathbf{M}_{16}$); six in which two rings flip ($\mathbf{M}_{13}$, $\mathbf{M}_{14}$, $\mathbf{M}_{15}$); four in which three rings flip ($\mathbf{M}_{12}$); and one in which all four rings flip ($\mathbf{M}_{11}$). The three different two-ring flips are distinguished in that the two flipping rings may be geminal ($\mathbf{M}_{13}$), anti ($\mathbf{M}_{14}$), or gauche ($\mathbf{M}_{15}$). Note that only one idealized transition state structure corresponding to each of these seven modes is depicted in Figure 1.

We emphasize again that no direct information whatever is available on the structure of the transition state or of any other species along the reaction coordinate; the term "mechanism", as used in this paper, therefore refers exclusively to the permutational consequences, and to the energy requirements (barriers). The sketches in Figure 1 should therefore be regarded as no more than convenient idealizations.

It is appropriate to comment here on the physical significance of non-self-inverse double cosets,[5b,18] e.g., $\mathbf{M}_{15a}$ and $\mathbf{M}_{15b}$. Although the rearrangements belonging to inverse double cosets are different, they are grouped together since they are chemically indistinguishable, i.e., they cause the same site exchanges (since the permutations in one of the double cosets generate their inverses, which are in the inverse double coset) and they occur at the same rate. That is, the flip mechanisms associated with these double cosets have the same activation energies. In a $\mathbf{C}_2$ tetraarylethane there are two different sets of symmetry equivalent rings, which correspond to the two sets of gauche rings, and there are consequently two different sets of ring dihedral angles. Let the values of the ring dihedral angles be x and y. Then $\mathbf{M}_{15a}$ is the permutational consequence of the flip mechanism in which the rings with dihedral angle y flip and those with dihedral angle x nonflip, while in $\mathbf{M}_{15b}$ the rings with dihedral angle x flip and those with dihedral angle y nonflip. Thus, these are two distinct pathways. However, if all eight edges of the aryl rings are constitutionally identical, a starting structure yields the same final product by either $\mathbf{M}_{15a}$ or $\mathbf{M}_{15b}$, and goes through enantiomeric and therefore isoenergetic (in an achiral medium) transition states.

The seven modes discussed above apply rigorously only to those cases in which all four rings are the same and all have a local C_2 axis (i.e., the eight edges bear the same substituents). In this case, flip mechanisms which are represented by the same racemic mode[7] are indistinguishable in an achiral environment (i.e., they are rotationally equivalent or enantiomeric). Thus, there are only seven different (diastereomeric) flip mechanism transition states for TME. However, when the four rings are not all identical, some of the formerly mode equivalent pathways are now rendered diastereomeric. How many diastereomeric flip mechanism transition states are there for such a case, with all rings possessing a local C_2 axis? The permutations of the rings on a tetraarylethane skeleton, which are indistinguishable in an achiral environment, form the group $\mathbf{S}_2 \times \mathbf{S}_2 \simeq \mathbf{C}_{2h}$, where the first $\mathbf{S}_2$ corresponds to a C_2 rotation and the second to a reflection (enantiomerization). In order to determine the number of idealized diastereomeric transition states (N_j) within a given mode ($\mathbf{M}_j$), it is convenient to use the formula:[7]

$$Z = \frac{|\mathbf{G}|}{|\mathbf{A}||\mathbf{B}|} \sum_{r=1}^{k} \frac{|\mathbf{A} \cap \mathbf{C}_r| \, |\mathbf{B} \cap \mathbf{C}_r|}{|\mathbf{C}_r|} \qquad (1)$$

where $Z = N_j$, $\mathbf{G} = \mathbf{S}_2 \times \mathbf{S}_2 \simeq \mathbf{C}_{2h}$, $\mathbf{A}$ is the point group of the idealized TPE transition state, $\mathbf{B}$ is the subgroup of $\mathbf{G}$ containing permutations of constitutionally identical ligands (rings), and $\mathbf{C}_r$ is one of the k conjugacy classes of $\mathbf{G}$ ($k = 4$ for $\mathbf{G} \simeq \mathbf{C}_{2h}$).

The total number of diastereomeric transition states is ΣN_j, summed over all modes ($\mathbf{M}_j$, $j = 11$–17). Thus, for a tetraarylethane with two constitutionally identical chiral centers (i.e., of type *ab*CHCH*ab*), when all four rings possess local C_2 axes there will be ten diastereomeric transition states for the racemic configuration ($\mathbf{B} = \mathbf{C}_2$) and ten for the meso configuration ($\mathbf{B} = \mathbf{C}_i$).

Although various substitution patterns may lower the symmetry of the molecule relative to the skeletal symmetry, and thus render mode equivalent pathways diastereomeric, the full power of a modal analysis lies in the assumption that the chemical perturbations introduced by substituting the skeleton with different ligands are small enough[18] so that there is no interdigitation of the activation energy levels of pathways belonging to different modes. That is, although there may be diastereomeric pathways within each of the several modes, if the difference in the ligands is small enough, the activation energies required for all the pathways in one mode will be lower than for all the pathways in another mode. Throughout this paper, this assumption underlies our analysis of rearrangement pathways.

Threshold Mechanism in Tetraarylethanes

DNMR Analysis of TME. When a hexachloro-1,3-butadiene solution of TME is warmed, the six methyl signals in the ^{1}H NMR spectrum, numbered 1 through 6 in Figure 2, pairwise coalesce, and at 170° only three singlets due to TME are observed in the methyl region of the spectrum. Two of these signals correspond to the ortho methyl groups, while the remaining one is attributable to the para methyl groups. The Gutowsky-Holm approximation,[19] in conjunction with the Eyring equation, yields $\Delta G^{\ddagger}_{134} = 22.8$ kcal/mol from the coalescence of signals 5 and 6. Analogously, the coalescence of signals 3 and 4 and of 1 and 2 yields $\Delta G^{\ddagger}_{138} = 22.2$ and $\Delta G^{\ddagger}_{155} = 22.9$ kcal/mol, respectively. These values are all the same within experimental error ($\Delta G^{\ddagger}$ data from coalescence of signals 3 and 4 are believed to be less accurate because of a small temperature dependence of the chemical shift of these two signals), indicating that only one process is responsible for the coalescence of the six signals to three. Increasing the temperature above 170° causes extensive decomposition (not surprisingly, since homolysis of TME has been reported to occur at high temperatures[20]), and even at 170° signals due to the decomposition product are already in evidence (asterisked peaks in Figure 2). Thus, higher temperature DNMR analysis of TME is precluded.

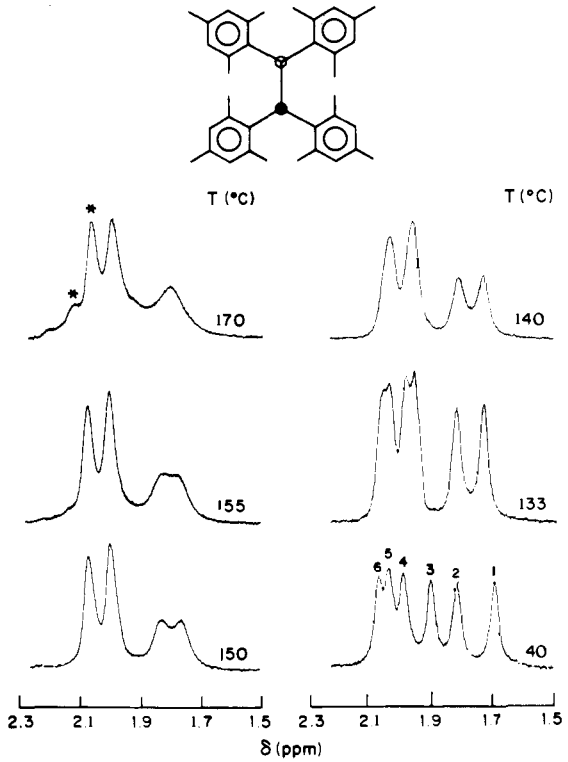

Figure 2. Temperature-dependent (methyl region) 60-MHz ^{1}H NMR spectrum of TME in hexachloro-1,3-butadiene. The asterisked peaks in the 170 °C spectrum represent absorptions due to the decomposition product.

To explain why the four ortho methyl signals coalesce pairwise to two, rather than to one singlet, it will be helpful to consult Figure 3, a graph in which the edges denote stereoisomerization pathways of TME, and the two vertices represent the two enantiomeric forms of TME. Each of the seven diastereomeric flip mechanisms (corresponding to the seven rearrangement modes $\mathbf{M}_{11}$–$\mathbf{M}_{17}$) results in enantiomerization (since helicity is reversed), whereas inversion at the central carbon atoms alone does not (and hence is strictly a topomerization). Thus, an optically active sample of TME would be racemized by any of the flip mechanisms, but not by inversion.

Examination of Figure 3 reveals that enantiomerization by one-, two-, or three-ring flip pathways ($\mathbf{M}_{12}$–$\mathbf{M}_{16}$) will result in a collapse of the four ortho methyl signals to a singlet, whereas the zero- ($\mathbf{M}_{17}$) and four-ring ($\mathbf{M}_{11}$) flips, as well as central inversion, will result in pairwise coalescence of the ortho and para methyl signals, as observed. This leaves the zero- and four-ring flip and central inversion as the only viable alternatives for the stereoisomerization pathway of lowest energy (threshold mechanism).

It is not possible to differentiate among these three mechanistic alternatives on the basis of DNMR alone. However, it is evident that the zero-ring flip requires an unacceptable degree of steric compression in the transition state, as compared to the four-ring flip. Furthermore, inversion does not seem to be a likely process.[21] Although observation of decomposition products above the coalescence temperature implies some dissociation, homolysis of TME has been shown to lead *irreversibly* to a radical-quinoid dimer equilibrium.[20] A dissociative mechanism would therefore not result in *stereo*isomerization. This conclusion is supported by evidence obtained on **1**; see below. Accordingly, we are left with the four-ring flip ($\mathbf{M}_{11}$) as the most likely explanation for the experimental results. It is intriguing to note that the threshold barrier (ca. 22.8 kcal/mol) falls within the range (22–23 kcal/mol) of values for the stereoisomerization of triarylmethanes in which the two

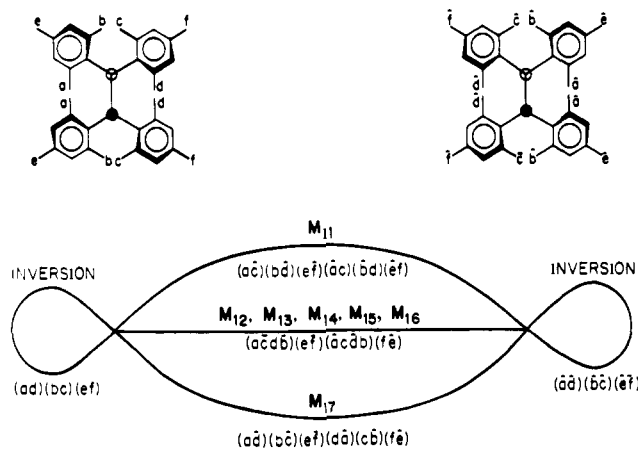

Figure 3. Topological representation of the possible stereoisomerizations of TME. The environments of the methyl groups are labeled with lower case letters. A barred letter denotes an enantiomeric environment. Exchanged (permuted) sites are parenthesized.

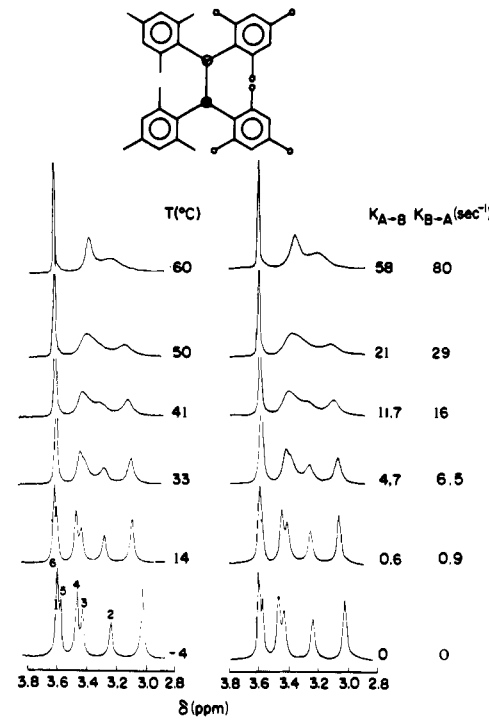

Figure 4. Temperature-dependent 60-MHz ^{1}H NMR spectrum (methoxy region) of racemic **1** in chloroform (left), and corresponding calculated spectra (right).

flipping rings are mesityl or 2,6-xylyl,[6] suggesting the possibility that the four-ring flip can be viewed as a composite of two two-ring flips.

Threshold Mechanism for Racemic 1. When a $CDCl_3$ solution of racemic **1** (see structures AĀ and BB̄ in Figure 4 of part 1 and note that in part 1 this compound is **2**) is heated, the six signals of unequal intensities in the methoxy region of the ^{1}H NMR spectrum broaden and ultimately coalesce to three signals of equal intensity (Figure 4). This coalescence process must be due to conformational diastereomerization, i.e., A ⇄ B and Ā ⇄ B̄. Complete line-shape analysis of the NMR tracings was performed[22] and a satisfactory match between the calculated and experimental spectra at five temperatures was obtained (Figure 4) by constructing a probability matrix in which signals 1 and 3, 2 and 4, and 5 and 6 were allowed to undergo mutual exchange. The rate data determined by line-shape analysis were used to calculate free energy parameters

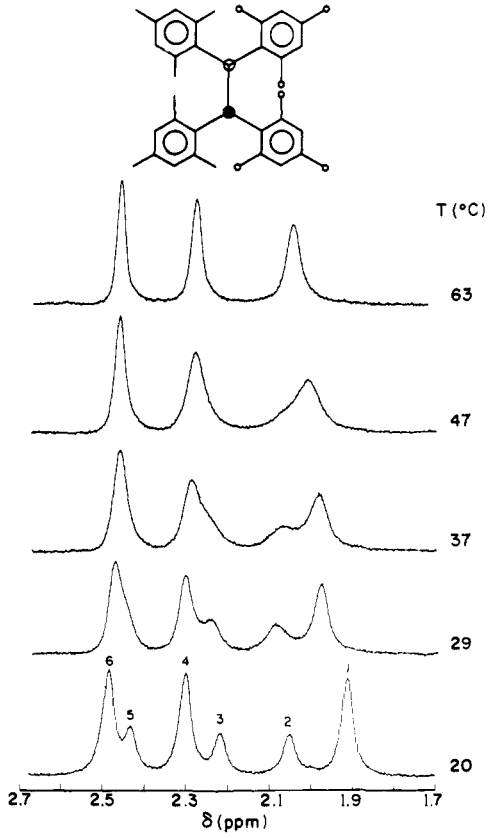

Figure 5. Temperature-dependent 60-MHz ^{1}H NMR spectrum of racemic **1** (methyl region) in chlorobenzene.

for the diastereomerization process: $\Delta G°_{20}$ = 0.18 kcal/mol for the equilibrium $A\bar{A} \rightleftarrows B\bar{B}$ (A was arbitrarily assumed to be the more stable isomer), $\Delta G^{\ddagger}_{40}$ = 17.0 kcal/mol for the reaction $A\bar{A} \rightarrow B\bar{B}$, and $\Delta G^{\ddagger}_{40}$ = 16.8 kcal/mol for the reverse reaction.

A conformational diastereomerization process is also observed in the methyl region (Figure 5). When a chlorobenzene solution of racemic **1** is warmed, signals 1 and 2, 3 and 4, and 5 and 6 pairwise coalesce at 29, 37, and 47°, respectively, to yield three signals of equal intensity. From the coalescence temperatures, the chemical shift differences, and the population ratio of the two diastereomers,[2] an average $\Delta G^{\ddagger}$ of 17.3 kcal/mol was calculated[23] for the process $A\bar{A} \rightarrow B\bar{B}$, and a $\Delta G^{\ddagger}$ of 16.8 kcal/mol for the reverse reaction.

Since the diastereomerization barriers determined from the methyl and methoxy signal coalescences are the same, we conclude that a single diastereoisomerization process is responsible for both sets of observations. It remains to determine which rearrangement modes are consistent with the observed site exchanges.

For racemic **1** there are ten diastereomeric flip mechanisms (see above) which inolve helicity reversal (i.e., which are within $\mathbf{M}_{11}$-$\mathbf{M}_{17}$), and which interconvert the two diastereomeric forms. These are listed in Table II. We note that enantiomerization (i.e., $A \rightleftarrows \bar{A}$ and $B \rightleftarrows \bar{B}$) requires inversion at *both* chiral centers and may therefore be safely eliminated from consideration: inversion is not a feasible rearrangement for these compounds under the conditions of the experiment as seen by lack of interconversion of racemic **1** and *meso*-**1** (inversion at one center) and by the absence of observable decomposition products.

From Table II it is evident that only four of the flip mechanisms are consistent with the low temperature process observed for racemic **1**, i.e., only the zero-, (1,3)-, (2,4)-, and (1,2,3,4)-ring flips average *both* the six methyl and the six

Table II. Effect of Diastereomerization Processes on the Environments of the Methoxy and Methyl Groups in Racemic **1**[a]

Flip pathways	Associated mode	Resulting exchanges[b] Methyl	Methoxy
(Zero)	$\mathbf{M}_{17}$	[ad][be][cf]	[gj][hk][il]
(1) or (3)[c]	$\mathbf{M}_{16}$	[abde][cf]	[gj][hk][il]
(2) or (4)[c]	$\mathbf{M}_{16}$	[ad][be][cf]	[ghkj][il]
(1,2) or (3,4)[c]	$\mathbf{M}_{13}$	[abde][cf]	[ghkj][il]
(1,4) or (2,3)[c]	$\mathbf{M}_{14}$	[abde][cf]	[ghkj][il]
(1,3)	$\mathbf{M}_{15}$	[ae][bd][cf]	[gj][hk][il]
(2,4)	$\mathbf{M}_{15}$	[ad][be][cf]	[gk][hj][il]
(1,2,4) or (2,3,4)[c]	$\mathbf{M}_{12}$	[abde][cf]	[gk][hj][il]
(1,2,3) or (1,3,4)[c]	$\mathbf{M}_{12}$	[ae][bd][cf]	[ghkj][il]
(1,2,3,4)	$\mathbf{M}_{11}$	[ae][bd][cf]	[gk][hj][il]

[a] See Figure 4 in part I for explanation of numerals and letters. Diastereomerization signifies $A \rightleftarrows B$ and $\bar{A} \rightleftarrows \bar{B}$. [b] Lower case letters in brackets designate methoxy or methyl groups whose environments are averaged by the process indicated. [c] These processes are rotationally equivalent.

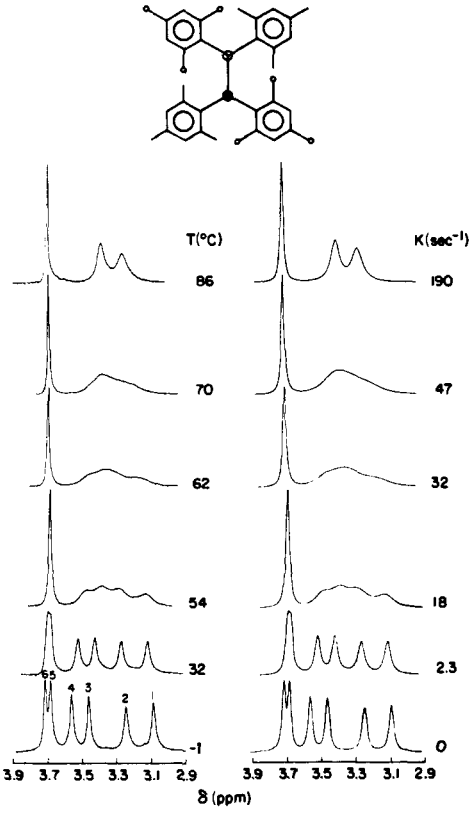

Figure 6. Temperature-dependent 60-MHz ^{1}H NMR spectrum (methoxy region) of *meso*-**1** in chloroform (left), and corresponding calculated spectra (right).

methoxy signals pairwise to three signals, each of equal intensity. A rigorous distinction among these four alternative pathways is not possible at this time since we cannot identify the specific groups which undergo site exchange, i.e., we cannot differentiate between [ad][be] and [ae][bd], or between [gj][hk] and [gk][hj]. However, since the threshold mechanism for TME was found to be the (1,2,3,4)-ring flip ($\mathbf{M}_{11}$), we feel justified in tentatively assigning the same mechanism to the diastereomerization of racemic **1**.

Threshold Mechanism for *meso*-1. When a $CDCl_3$ solution of *meso*-**1** (see structures C and $\bar{C}$ in Figure 5 of part 1) is warmed, the six signals of equal intensity in the methoxy region of the ^{1}H NMR spectrum[2] broaden, and ultimately coalesce to three signals of equal intensity (Figure 6). Stereoisomeri-

zation is evidently occurring on the NMR time scale, and since we have already discounted inversion as a feasible operation under the conditions of our experiment, this coalescence must be due to conformational enantiomerization, i.e., C ⇄ C̄. A satisfactory fit between experimental and simulated spectra (Figure 6) was obtained[22] by constructing a probability matrix in which signals 1 and 3, 2 and 4, and 5 and 6 were allowed to undergo mutual exchange. From the rate data determined by line-shape analysis, a value of $\Delta G^{\ddagger}_{50}$ = 17.3 kcal/mol was found for the enantiomerization.

As noted in part 1, *meso*-**1** exhibits only four signals in the methyl region of the ^{1}H NMR spectrum in chlorobenzene solution at −11 °C (Figure 9, part 1), due to accidental isochronies. Coalescence of the two signals at highest field was found to occur at 49°, from which $\Delta G^{\ddagger}_{49}$ = 17.2 kcal/mol was calculated.[19] Thus, the energetics involved in both coalescences are the same, and once again we conclude that a single stereoisomerization process is responsible for both sets of observations.

Table III lists the environments of the methyl and methoxy groups of *meso*-**1**, which are exchanged by each of the ten diastereomeric flip mechanisms. Several sets of mode equivalent pathways are enantiomeric, and thus will necessarily occur at identical rates in an achiral medium; the results of interconversions by these pathways can therefore be considered together. Inspection of the effect of the ten different flip mechanisms (Table III) reveals that only four mechanisms (i.e., the zero-, (1,4)-, (2,3)-, and (1,2,3,4)-ring flips) are consistent with the low energy process observed for *meso*-**1**, i.e., the pairwise coalescence of *both* the methyl and methoxy signals to three equally intense peaks. Recalling the arguments previously invoked for TME and racemic **1**, we favor the (1,2,3,4)-ring flip ($\mathbf{M}_{11}$) as the threshold mechanism for *meso*-**1** as well.

A further argument may be adduced in support of the choice of $\mathbf{M}_{11}$ as the threshold rearrangement mode in tetraarylethanes. $\mathbf{M}_{11}$ and $\mathbf{M}_{17}$ are the only modes which are capable of accounting for the threshold processes observed for *both* racemic and meso forms of **1** (Tables II and III). Since the two stereoisomerizations occur with virtually identical activation energies ($\Delta G^{\ddagger}$ = 17 kcal/mol), and since the zero-ring flip ($\mathbf{M}_{17}$) requires very different nonbonded interactions for the isomers, it naturally follows that the four-ring flip ($\mathbf{M}_{11}$), for which the interactions are of comparable magnitude, remains as the only alternative.[24]

In summary, the present body of work on TME and **1** suggests the generalization that the four-ring flip is the threshold mechanism in tetraarylethanes, provided that the two edges of each aryl ring do not differ appreciably in steric congestion.

It will have been observed that for both stereoisomers of **1**, as well as for TME, the threshold mechanism ($\mathbf{M}_{11}$) is incapable of averaging the four ortho signals to a singlet. This observation is another manifestation of residual diastereotopism,[4,6] a phenomenon previously encountered in the analysis of complex triarylmethanes[4,25] and triarylamines,[27] and which owes its existence to correlated rotation of the aryl rings.[4,6] An easy way to visualize the phenomenon in the present case is to picture the time-averaged structure of TME under the four-ring flip: such a structure has C_{2h} symmetry (see $\mathbf{M}_{11}$, Figure 1). This guarantees the symmetry equivalence of the para mesityl groups (one signal), but the ortho methyl groups fall into two symmetry nonequivalent sets of four each: the proximal (to methine hydrogens) and the distal. Similar considerations apply to **1**. The coalescence behavior of these residual signals will be discussed in the next section.

Table III. Effect of Enantiomerization Processes on the Environments of the Methoxy and Methyl Groups in *meso*-**1**[a]

Flip pathways	Associated mode	Resulting exchanges[b]	
		Methyl	Methoxy
(Zero)	$\mathbf{M}_{17}$	[aē][bd̄][cf̄] [āe][b̄d][c̄f]	[gk̄][hj̄][il̄] [ḡk][h̄j][ī l]
(1) and (4)[c]	$\mathbf{M}_{16}$	[abdē][cf̄] [āb̄de][c̄f]	[gk̄][hj̄][il̄] [ḡk][h̄j][ī l]
(2) and (3)[c]	$\mathbf{M}_{16}$	[aē][bd̄][cf̄] [āe][b̄d][c̄f]	[ghk̄j̄][il̄] [ḡhkj][ī l]
(1,2) and (3,4)[c]	$\mathbf{M}_{13}$	[abdē][cf̄] [āb̄de][c̄f]	[ghk̄j̄][il̄] [ḡhkj][ī l]
(1,4)	$\mathbf{M}_{14}$	[ad̄][bē][cf̄] [ād][b̄e][c̄f]	[gk̄][hj̄][il̄] [ḡk][h̄j][ī l]
(2,3)	$\mathbf{M}_{14}$	[aē][bd̄][cf̄] [āe][b̄d][c̄f]	[gj̄][hk̄][il̄] [ḡj][h̄k][ī l]
(1,3) and (2,4)[c]	$\mathbf{M}_{15}$	[abdē][cf̄] [āb̄de][c̄f]	[ghk̄j̄][il̄] [ḡhkj][ī l]
(1,2,3) and (2,3,4)[c]	$\mathbf{M}_{12}$	[abdē][cf̄] [āb̄de][c̄f]	[gj̄][hk̄][il̄] [ḡj][h̄k][ī l]
(1,2,4) and (1,3,4)[c]	$\mathbf{M}_{12}$	[ad̄][bē][cf̄] [ād][b̄e][c̄f]	[ghk̄j̄][il̄] [ḡhkj][ī l]
(1,2,3,4)	$\mathbf{M}_{11}$	[ad̄][bē][cf̄] [ād][b̄e][c̄f]	[gj̄][hk̄][il̄] [ḡj][h̄k][ī l]

[a] See Figure 5 in part I for explanation of numerals and letters. Enantiomerization signifies C ⇄ C̄. [b] Lower case letters in brackets designate methoxy or methyl groups whose environments are averaged by the process indicated. [c] These processes are enantiomeric.

Higher Energy Processes

The ^{1}H NMR spectrum of TME at 170° (Figure 2) clearly shows that the ortho methyl groups still reside in diastereomeric environments, even though the enantiomerization process at that temperature is fast on the NMR time scale. In order to site exchange these residually diastereotopic ortho methyl groups, a pathway different from the four-ring flip must be traversed. However, since a combination of the four-ring flip with any one of the other pathways listed in Figure 3 suffices to average these signals, no further information can be gained concerning the identity of any high energy process, even if coalescence of the residual signals could be experimentally detected. We therefore turned our attention to **1**, in which some of the degeneracies inherent in TME have been removed by the replacement of two of the mesityl groups by two 2,4,6-trimethoxyphenyl groups.

At 78°, the ^{1}H NMR spectrum of racemic **1** in 1,2,4-trichlorobenzene (Figure 7) clearly reveals the residual diastereotopism of the ortho methyl and ortho methoxy groups (cf. also Figures 4 and 5). At this temperature, diastereomerization (AĀ ⇄ BB̄) proceeds rapidly on the NMR time scale. Upon further heating, the downfield (ortho methoxy) signals are seen (Figure 7) to coalesce at 97°; for this exchange process, a $\Delta G^{\ddagger}_{97}$ of 19.8 kcal/mol was calculated.[19] Coalescence of the upfield (ortho methyl) signals occurs at 165°, and for this process a $\Delta G^{\ddagger}_{165}$ for 23.1 kcal/mol was calculated.[19] We conclude from the difference in energy of the two processes that two different (diastereomeric) isomerization pathways must be involved, one of which averages the methoxy signals, while the other averages the methyl signals.

Since the threshold mechanism ($\mathbf{M}_{11}$) is incapable of exchanging the sites of distal and proximal ortho methyl or methoxy groups, and thus of averaging the residual set of signals, pathways other than the four-ring flip must be traversed. Given that the two transition states for the observed higher energy processes must be diastereomeric, only pathways 6-9 (Table IV) need be taken under consideration. For the exchange of the residually diastereotopic methoxy groups, either a combination of four- and two-ring flips ($\mathbf{M}_{11} + \mathbf{M}_{15}$, pathway 6) or a combination of four- and three-ring flips ($\mathbf{M}_{11} + \mathbf{M}_{12}$, pathway 9) could account for the observed coalescence at 97°. Either the mode equivalent pathway 7 ($\mathbf{M}_{11} + \mathbf{M}_{15}$) or path-

Table IV. Effect of Diastereomerization Processes on the Environments of the Methoxy and Methyl Groups in Racemic **1**[a]

No.	Flip pathways	Associated mode	Resulting exchanges[b]	
			Methyl	Methoxy
1	(1,2,3,4) + (zero)	$\mathbf{M}_{11} + \mathbf{M}_{17}$	[abde][cf]	[ghkj][il]
2	(1,2,3,4) + (1) or (3)	$\mathbf{M}_{11} + \mathbf{M}_{16}$	[abde][cf]	[ghkj][il]
3	(1,2,3,4) + (2) or (4)	$\mathbf{M}_{11} + \mathbf{M}_{16}$	[abde][cf]	[ghkj][il]
4	(1,2,3,4) + (1,2) or (3,4)	$\mathbf{M}_{11} + \mathbf{M}_{13}$	[abde][cf]	[ghkj][il]
5	(1,2,3,4) + (1,4) or (2,3)	$\mathbf{M}_{11} + \mathbf{M}_{14}$	[abde][cf]	[ghkj][il]
6	(1,2,3,4) + (1,3)	$\mathbf{M}_{11} + \mathbf{M}_{15}$	[ae][bd][cf]	[ghkj][il]
7	(1,2,3,4) + (2,4)	$\mathbf{M}_{11} + \mathbf{M}_{15}$	[abde][cf]	[gk][hj][il]
8	(1,2,3,4) + (1,2,4) or (2,3,4)	$\mathbf{M}_{11} + \mathbf{M}_{12}$	[abde][cf]	[gk][hj][il]
9	(1,2,3,4) + (1,2,3) or (1,3,4)	$\mathbf{M}_{11} + \mathbf{M}_{12}$	[ae][bd][cf]	[ghkj][il]

[a,b] Footnotes correspond to those in Table II.

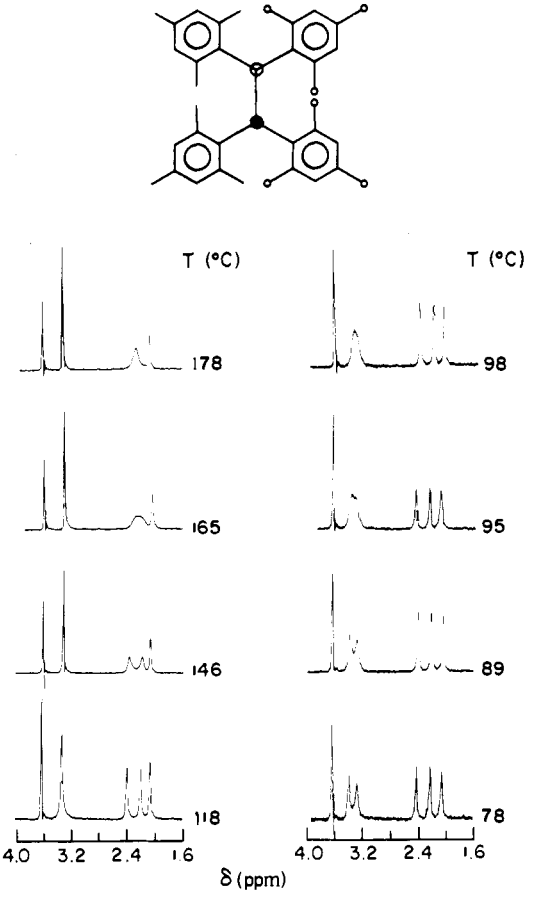

Figure 7. Temperature-dependent 60-MHz ^{1}H NMR spectrum of racemic **1** (methyl and methoxy regions) in 1,2,4-trichlorobenzene.

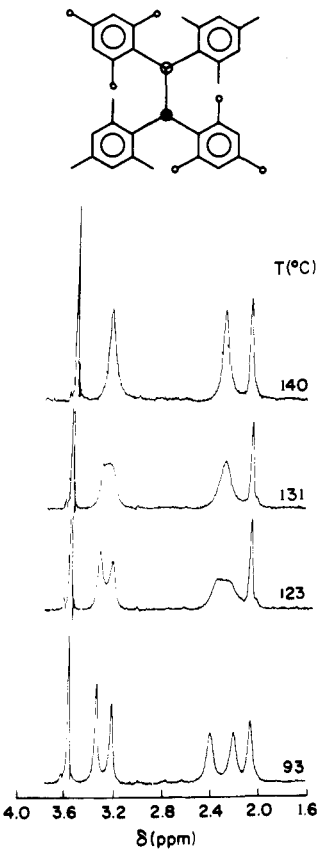

Figure 8. Temperature-dependent 60-MHz ^{1}H NMR spectrum of *meso*-**1** (methyl and methoxy regions) in 1,2,4-trichlorobenzene.

way 8 ($\mathbf{M}_{11} + \mathbf{M}_{12}$), respectively, would then account for the coalescence of the methyl group signals at 165°. In contradistinction, a combination of $\mathbf{M}_{11}$ with any of the other modes (pathways 1-5, Table IV) would simultaneously average (isoenergetic coalescence) both sets of signals due to residually diastereotopic ortho methoxy and ortho methyl groups, contrary to the observation of *two* higher barriers. Consequently, these other pathways can be safely dismissed from consideration.

The ^{1}H NMR spectrum of *meso*-**1** in 1,2,4-trichlorobenzene at 93° exhibits three equally intense signals in the methyl as well as in the methoxy region (Figure 8), evidence for the residual diastereotopism of the ortho methyl and ortho methoxy groups. At that temperature, enantiomerization (C $\rightleftarrows$ $\bar{\text{C}}$) proceeds rapidly on the NMR time scale. At higher temperatures, these signals coalesce to singlets. Coalescence of the ortho methyl and methoxy signals occurs at 123 and 131°, respectively, from which values of $\Delta G^{\ddagger}_{123} = 20.8$ and $\Delta G^{\ddagger}_{131} = 21.5$ kcal/mol were calculated.[19] Although the difference between the two barriers (0.7 kcal/mol) is smaller than was the case for racemic **1** (3.3 kcal/mol), it is clear that once again two different (diastereomeric) pathways must be implicated. Only pathways 6-9 (Table V) need be considered. Either a combination of four- and two-ring flips ($\mathbf{M}_{11} + \mathbf{M}_{14}$, pathway 7) or of four- and three-ring flips ($\mathbf{M}_{11} + \mathbf{M}_{12}$, pathway 8) could account for the coalescence of methyl signals at 123°, and either the mode equivalent pathway 6 ($\mathbf{M}_{11} + \mathbf{M}_{14}$) or pathway 9 ($\mathbf{M}_{11} + \mathbf{M}_{12}$), respectively, would then account for the coalescence of methoxy signals at 131°. Any combination of $\mathbf{M}_{11}$ with $\mathbf{M}_{13}$, $\mathbf{M}_{15}$, $\mathbf{M}_{16}$, or $\mathbf{M}_{17}$ would lead to simultaneous averaging of the methyl and methoxy signals (pathways 1-5, Table V), contrary to observation.

Table V. Effect of Enantiomerization Processes on the Environments of the Methoxy and Methyl Groups in *meso*-**1**[a]

No.	Flip pathways	Associated mode	Resulting exchanges[b]	
			Methyl	Methoxy
1	(1,2,3,4) + (zero)	$\mathbf{M}_{11} + \mathbf{M}_{17}$	[abd̄ē][cf̄] [ād̄bē][c̄f] [abd̄ē][cf̄]	[ghk̄j̄][il̄] [g̃h̃kj][ĩl̃] [ghk̄j̄][il̄]
2	(1,2,3,4) + (1) and (4)	$\mathbf{M}_{11} + \mathbf{M}_{16}$	[ād̄bē][c̄f] [abd̄ē][cf̄] [ād̄bē][c̄f]	[g̃h̃kj][ĩl̃] [ghk̄j̄][il̄] [g̃h̃kj][ĩl̃]
3	(1,2,3,4) + (2) and (3)	$\mathbf{M}_{11} + \mathbf{M}_{16}$	[abd̄ē][cf̄] [ād̄bē][c̄f] [abd̄ē][cf̄]	[ghk̄j̄][il̄] [g̃h̃kj][ĩl̃] [ghk̄j̄][il̄]
4	(1,2,3,4) + (1,2) and (3,4)	$\mathbf{M}_{11} + \mathbf{M}_{13}$	[ād̄bē][c̄f] [abd̄ē][cf̄] [ād̄bē][c̄f]	[g̃h̃kj][ĩl̃] [ghk̄j̄][il̄] [g̃h̃kj][ĩl̃]
5	(1,2,3,4) + (1,3) and (2,4)	$\mathbf{M}_{11} + \mathbf{M}_{15}$	[abd̄ē][cf̄] [ād̄bē][c̄f] [abd̄ē][cf̄]	[ghk̄j̄][il̄] [g̃h̃kj][ĩl̃] [ghk̄j̄][il̄]
6	(1,2,3,4) + (1,4)	$\mathbf{M}_{11} + \mathbf{M}_{14}$	[ad̄][bē][cf̄] [ād̄][b̄e][c̄f] [abd̄ē][cf̄]	[ghk̄j̄][il̄] [g̃h̃kj][ĩl̃] [gj̄][hk̄][il̄]
7	(1,2,3,4) + (2,3)	$\mathbf{M}_{11} + \mathbf{M}_{14}$	[ād̄bē][c̄f] [abd̄ē][cf̄] [ād̄bē][c̄f]	[g̃j̃][h̃k̃][ĩl̃] [gj̄][hk̄][il̄] [g̃j̃][h̃k̃][ĩl̃]
8	(1,2,3,4) + (1,2,3) and (2,3,4)	$\mathbf{M}_{11} + \mathbf{M}_{12}$	[abd̄ē][cf̄] [ād̄bē][c̄f]	[gj̄][hk̄][il̄] [g̃j̃][h̃k̃][ĩl̃]
9	(1,2,3,4) + (1,2,4) and (1,3,4)	$\mathbf{M}_{11} + \mathbf{M}_{12}$	[ad̄][bē][cf̄] [ād̄][b̄e][c̄f]	[ghk̄j̄][il̄] [g̃h̃kj][ĩl̃]

[a,b] Footnotes correspond to those in Table III.

In summary: the site exchanges of diastereotopic methyl and methoxy groups in racemic and meso **1** take place by way of a two- or a three-ring flip in combination with a four-ring flip. However, the two-ring flip rearrangements in racemic and *meso*-**1** are mode-nonequivalent ($\mathbf{M}_{15}$ and $\mathbf{M}_{14}$, respectively).

Although a choice cannot be made at this time among these alternatives, we are attracted by the possibility that all of the higher barriers can be accounted for by rearrangements belonging to a single mode, $\mathbf{M}_{12}$, i.e., that the coalescence of the four ortho methyl and methoxy signals to a singlet is mainly (or even exclusively) due to a combination of four- and three-ring flips (pathways 8 and 9, Tables IV and V). The difference in energy between the methyl and methoxy site exchanges is the consequence, in this view, of the diastereoisomerism of pathways 8 (methyl) and 9 (methoxy). This hypothesis, which is admittedly quite speculative and yet remains to be experimentally verified, is appealing for two reasons. First, it has the virtue of simplicity, i.e., it is the most economic way of accounting for all of our observations and thus satisfies the demands of Ockham's razor. Second, since the four-ring flip is the threshold mechanism, it might seem intuitively reasonable to suppose that the next highest energy pathway would involve the flipping of three rings.

Residual Stereoisomerism and Residual Stereotopism

Other substitution patterns on the TPE skeleton provide additional information concerning the rearrangement modes (stereoisomerization pathways) associated with the higher energy processes. The number of stereoisomeric forms for variously substituted tetraarylethanes has been tabulated (part I). The indiscriminate removal of degeneracies in such systems is unlikely to lead to the desired goal; what is needed is a rational approach which allows a selection of the most informative examples. As will be shown, the group theoretical analysis of the dynamic stereochemistry of complex tetraarylethanes does, in fact, provide such an approach. The next sections are designed to illustrate how residual stereoisomerism and residual stereotopism in selected submaximally labeled structures can be used to determine the ordering of rearrangement modes which follow $\mathbf{M}_{11}$ in energy.

Subgroup Lattice. We shall make use of the lattice of subgroups[5b] between the point group ($\mathbf{C}_2$) and the feasible permutation-inversion group ($\mathbf{G}_{64}$). Since all of these subgroups contain intact modes,[5b] this lattice is derived by generating groups from each individual mode and from combinations of modes. The modes (Table I) contained in each subgroup of $\mathbf{G}_{64}$ are listed in Table VI.

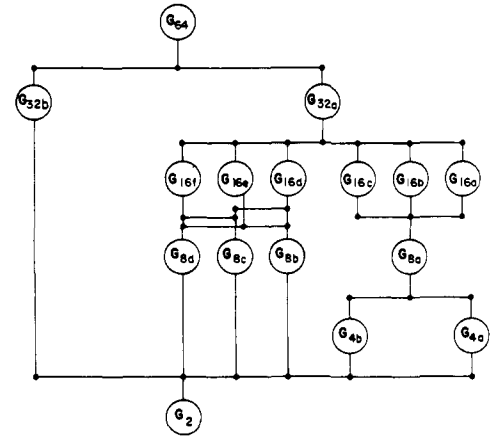

Figure 9. Lattice of subgroups between the point group ($\mathbf{C}_2$) and the feasible permutation-inversion group ($\mathbf{G}_{64}$) which contains elements resulting in a change of helicity (i.e., those in the $h\mathbf{R}_{32}$ coset). See Table VI for the modes contained in each subgroup.

The subgroup lattice provides information on the number of distinct observable processes. Since single-step isomerizations for tetraarylethanes are considered to involve a change in helicity, we show the lattice of only those subgroups which include one or more of modes $\mathbf{M}_{11}$–$\mathbf{M}_{17}$ (Figure 9). Each step on the lattice corresponds to "turning on" an additional process. Thus, to step from $\mathbf{G}_2$ to $\mathbf{G}_{4a}$ requires $\mathbf{M}_{11}$, from $\mathbf{G}_{4a}$ to $\mathbf{G}_{8a}$ requires $\mathbf{M}_{17}$, etc. It follows that the maximum number of mode nonequivalent processes which would be observed is five, corresponding, e.g., to the sequence:

$$\mathbf{G}_2 \xrightarrow{\mathbf{M}_{11}} \mathbf{G}_{4a} \xrightarrow{\mathbf{M}_{17}} \mathbf{G}_{8a} \xrightarrow{\mathbf{M}_{15}} \mathbf{G}_{16a} \xrightarrow{\mathbf{M}_{14}\text{ or }\mathbf{M}_{13}} \mathbf{G}_{32a} \xrightarrow{\mathbf{M}_{12}\text{ or }\mathbf{M}_{16}} \mathbf{G}_{64}$$

Fewer processes can be observed if the action of an additional mode skips a step in this sequence. For example, $\mathbf{M}_{11}$ followed by $\mathbf{M}_{12}$ corresponds to the sequence:

$$\mathbf{G}_2 \xrightarrow{\mathbf{M}_{11}} \mathbf{G}_{4a} \xrightarrow{\mathbf{M}_{12}} \mathbf{G}_{64}$$

Table VI. Subgroups of G_{64} Which Contain C_2[a]

	M_1	M_2	M_3	M_4	M_5	M_6	M_7	M_8	M_9	M_{10}	M_{11}	M_{12}	M_{13}	M_{14}	M_{15}	M_{16}	M_{17}
*G_{64}[b]	1	1	1	1	1	1	1	1	1	1	1	1	1	1	1	1	1
*G_{32a}	1	–	–	1	1	1	1	–	–	1	1	–	1	1	1	–	1
*G_{32b}	1	–	–	1	1	1	1	–	–	1	–	1	–	–	–	1	–
G_{32c}	1	1	1	1	1	1	1	1	1	1	–	–	–	–	–	–	–
*G_{16a}	1	–	–	–	–	1	1	–	–	1	1	–	–	–	1	–	1
*G_{16b}	1	–	–	–	1	–	–	–	–	1	1	–	–	1	–	–	1
*G_{16c}	1	–	–	1	–	–	–	–	–	1	1	–	1	–	–	–	1
*G_{16d}	1	–	–	–	1	–	–	–	–	1	–	–	1	–	1	–	–
*G_{16e}	1	–	–	1	–	–	–	–	–	1	–	–	–	1	1	–	–
*G_{16f}	1	–	–	–	–	1	1	–	–	1	–	–	1	1	–	–	–
G_{16g}	1	–	–	1	1	1	1	–	–	1	–	–	–	–	–	–	–
G_{16h}	1	–	1	–	–	1	1	–	1	1	–	–	–	–	–	–	–
G_{16i}	1	1	–	–	–	1	1	1	–	1	–	–	–	–	–	–	–
*G_{8a}	1	–	–	–	–	–	–	–	–	1	1	–	–	–	–	–	1
*G_{8b}	1	–	–	–	–	–	–	–	–	1	–	–	–	–	1	–	–
*G_{8c}	1	–	–	–	–	–	–	–	–	1	–	–	–	1	–	–	–
*G_{8d}	1	–	–	–	–	–	–	–	–	1	–	–	1	–	–	–	–
G_{8e}	1	–	–	–	1	–	–	–	–	1	–	–	–	–	–	–	–
G_{8f}	1	–	–	1	–	–	–	–	–	1	–	–	–	–	–	–	–
G_{8g}	1	–	–	–	–	–	1	–	1	–	–	–		–	–	–	–
G_{8h}	1	–	–	–	–	1	1	–	–	1	–	–	–	–	–	–	–
G_{8i}	1	–	1	–	–	–	1	–	–	–	–	–	–	–	–	–	–
G_{8j}	1	–	–	–	–	1	–	1	–	–	–	–	–	–	–	–	–
G_{8k}	1	–	–	–	1	–	–	–	–	–	–	–	–	–	–		
*G_{4a}	1	–	–	–	–	–	–	–	–	–	1	–	–	–	–	–	–
*G_{4b}	1	–	–	–	–	–	–	–	–	–	–	–	–	–	–	–	1
G_{4c}	1	–	–	–	–	–	–	–	–	1	–	–	–	–	–	–	–
G_{4d}	1	–	–	–	–	–	1	–	–	–	–	–	–	–	–	–	–
G_{4e}	1	–	–	–	–	1	–	–	–	–	–	–	–	–	–	–	–
G_2	1	–	–	–	–	–	–	–	–	–	–	–	–	–	–	–	–

[a] The subgroups were generated by use of the program referred to in footnote *b* of Table I. [b] Groups marked with an asterisk include permutations which change helicity and are displayed in the lattice of Figure 9.

and thus no other process can be observed, since the entire feasible permutation-inversion group has been generated.

Residual Stereoisomerism in Maximally Labeled Arylmethanes and Arylethanes. In the discussion of triarylmethanes we found it convenient to introduce the concept of residual stereoisomerism.[4,6] The skeletal point group in that case is C_3,[16a,28] a chiral group, and the full permutation-inversion group is therefore $S_3[S_2] \times C_{i*} = G_{96}$, of order 96.[5b] Thus, there are $|G_{96}|/|C_3| = 32$ isomers (16 with a given central configuration) in the maximally labeled case,[8] in which all rings are different and lack local C_2 axes. The threshold isomerization mechanism was found to be the two-ring flip,[16a,29] which corresponds to one of the modes of C_3 in G_{96}. The permutations in that mode generate only 24 elements of the group, and there are four sets, each consisting of eight conformational diastereomers, which are not interconverted by this mechanism and which constitute a set of residual stereoisomers (two *dl* pairs).[4,6] In general the number of residual isomers (Z) in the maximally labeled case can be found by use of a simplified version of eq 1 (where $|B| = 1$), i.e.:

$$Z = |G|/|A|$$

where **G** is the full permutation-inversion group and **A** is gp{M_j}, the group generated by the permutations in the modes which are occurring on the time scale of observation[7] (i.e., **A** is the smallest subgroup of **G** which contains those modes).[5b]

In the case of tetraarylmethanes, the threshold mechanism[30] corresponds to a mode which generates the entire feasible permutation group $A_4[S_2]$ (the full permutation group is $S_4[S_2]$).[5] Thus, even in a maximally labeled structure there are only $|S_4[S_2]|/|A_4[S_2]| = 2$ residual isomers, i.e., the one pair of conventional enantiomers whose isomerism is due to the presence of a chiral center.

As seen from Table VI, every mode for tetraarylethanes is contained in at least one proper subgroup of G_{64}. Since a mode will generate the subgroup of smallest order in which it is contained, it follows that no one mode generates the entire feasible permutation-inversion group (G_{64}). Thus, there *must* be residual stereoisomers above and beyond those arising from the presence of chiral centers if the threshold mechanism, whatever it might be, is the only isomerization mechanism occurring on the time scale of observation.

Results of DNMR experiments (see above) indicate that M_{11} is the threshold isomerization mode. Thus, in contrast to the paucity of residual stereoisomers in the polyarylmethanes, one can expect a plethora of residual stereoisomers in maximally labeled tetraarylethanes. For such a compound there would be $|G_{256}|/|gp\{M_{11}\}| = |G_{256}|/|G_{4a}| = 64$ residual stereoisomers (16 for each of the four conventional configurational stereoisomers, i.e., 32 *dl* pairs).

Residual Stereoisomerism in Submaximally Labeled Tetraarylethanes. To compute the number of residual stereoisomers (Z) in submaximally labeled molecules, one can make use of the formula[7] in eq 1, where **G** = full permutation-inversion group[2] (G_{256} for all configurations; $G_{128} = R_{64} \times C_{i*}$ for racemic or meso configurations for a skeleton of type *ab*-CHCH*ab*[31]); **A** = the "apparent" point group; **A** is being used in the general sense to include not only the usual point group operations of the TPE skeleton, but also any operation which is fast on the time scale of observation[5b,7] (e.g., a rearrangement mode) or which is not distinguishable (e.g., enantiomerization); **B** = subgroup of **G** containing permutations of nondifferentiable edges; C_r = one of the k conjugacy classes of **G** (see supplementary material for part 1).

The number of differentiable residual stereoisomers depends on whether the environment is chiral or achiral. If the environment is chiral, **A** = gp{M_j} is the smallest subgroup (see

Table VII. Classes of Substituted Tetraarylethanes with Constitutionally Symmetric Skeletons[a]

Class	Substitution pattern[b]	Total no. of isomers[c]	Chemical example[d]
I	4/4	2	$R_1R_1CH\text{-}CHR_1R_1$ (TME)
II	$2+2^e/4$	2	$R_1R_1CH\text{-}CHR_2R_2$ (**2**)
III	$2+2^f/4$	4/2	$R_1R_2CH\text{-}CHR_1R_2$ (**1**)
IV	$2+2^e/2$	8	$R_2R_2CH\text{-}CHR_3R_3$ (**3**)
V	$2+2^f/2$	12/8	$R_2R_3CH\text{-}CHR_2R_3$ (**4**)
VI	4/0	20	$R_4R_4CH\text{-}CHR_4R_4$ (**5**)
VII	$2+2^e/0$	32	$R_3R_3CH\text{-}CHR_4R_4$ (**6**)
VIII	$2+2^f/0$	40/32	$R_3R_4CH\text{-}CHR_3R_4$ (**7**)

[a] For substitution patterns a_2CHCHa_2, a_2CHCHb_2, and ab-CHCHab. [b] Notation: number of constitutionally identical rings/number of rings with a local C_2 axis. [c] See Table I of part I. Notation: number of isomers with racemic configuration/number of isomers with meso configuration. [d] R_1 = mesityl; R_2 = 2,4,6-trimethoxyphenyl; R_3 = 2-methylnaphthyl; R_4 = 2-methoxynaphthyl. [e] Systems with no chiral centers (a_2CHCHb_2). [f] Systems (racemic and meso) with two constitutionally identical chiral centers (abCHCHab).

Table VI) of G_{64} containing all those modes.[5b] Since enantiomers are not differentiable in an achiral environment, one calculates the number of isomers in such an environment by including in **A** the operation corresponding to a reflection, i.e., $(15)(26)(37)(48)^* = C_2^*$. Thus $\mathbf{A} = gp\{M_j\} \times \mathbf{C}_2^*$, where $\mathbf{C}_2^*$ is the group of order 2 generated by the operation C_2^*.

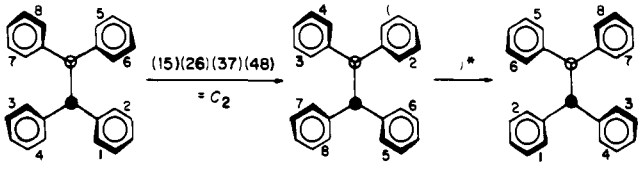

Design of Systems Suitable for Discriminating among Mechanistic Alternatives. It was previously shown that knowledge of the energetics of isomerization pathways can be used to predict the number and kinds of residual stereoisomers and number of signals due to residual diastereotopism.[4,6] We shall demonstrate that, conversely, the number and kind of residual stereoisomers or the number of signals due to residual diastereotopism can be used to determine the relative energetics of competing isomerization pathways.

In order to determine which substitution patterns are the most informative for the purpose of determining the second lowest energy pathway, we select those which give rise to the fewest degeneracies in the number and kind of isomers, calculated as described above, under the action of each mode in combination with $\mathbf{M}_{11}$, the threshold mechanism. We were thus led to concentrate our attention on the three skeletal types which are constitutionally symmetrical, i.e., a_2CHCHa_2, a_2CHCHb_2, and abCHCHab. These skeletal types are intuitively appealing for two reasons. First, they include the only ones capable of existing in forms with $\mathbf{C}_2$ symmetry (a_2CHCHa_2 and racemic abCHCHab). Second, they include the only ones which can enantiomerize by a flip mechanism (a_2CHCHa_2, a_2CHCHb_2, meso abCHCHab). There are eight classes of substitution patterns within these three general skeletal types; these classes and possible chemical examples are listed in Table VII.

A large variety of possible chemical realizations of each class can be envisaged; examples for classes I (TME) and III (**1**) have already been discussed. It is evident that the choice of a particular compound is tied to the time scale of observation under the conditions of the experiment. Thus, in order to separate residual stereoisomers under ordinary conditions, the barriers to interconversion should be no less than 25 kcal/mol, whereas this figure represents an upper limit if one is to extract information from DNMR measurements by the observation of residual stereotopism. Consequently, since the choice of a particular chemical structure is dictated by the method of investigation, it becomes necessary to determine which of the two approaches is the method of choice.

Three advantages of DNMR as compared to isomer separation are (1) the relatively greater ease of obtaining data (i.e., variable temperature NMR vs. isomer separation); (2) the greater number of NMR signals relative to the number of isomers (residual diastereotopism can be observed in systems which do not exhibit residual stereoisomerism,[4,6] as, for example, in the case of the enantiomerization of TME and *meso*-**1** under $\mathbf{M}_{11}$); (3) the relative ease of distinguishing diastereomeric pathways differing only slightly in activation energy. Two disadvantages of DNMR as compared to isomer separation are (1) the possibility of accidental isochronies; (2) different numbers and types of residual stereoisomers may give rise to the same number of signals.

The numbers and types of residual stereoisomers under the action of various modes are given in Scheme I, which provides a flow chart of stereoisomerizations under the action of $\mathbf{M}_{11}$ with any single subsequent mode ($\mathbf{M}_{12}$-$\mathbf{M}_{17}$) for classes IV-VIII. The results of the actions of various modes on the number of diastereotopic groups, and hence on the number of distinct NMR signals, is shown in Scheme II by the use of the specific examples listed in Table VII.

Scheme I[a]

Class[b]

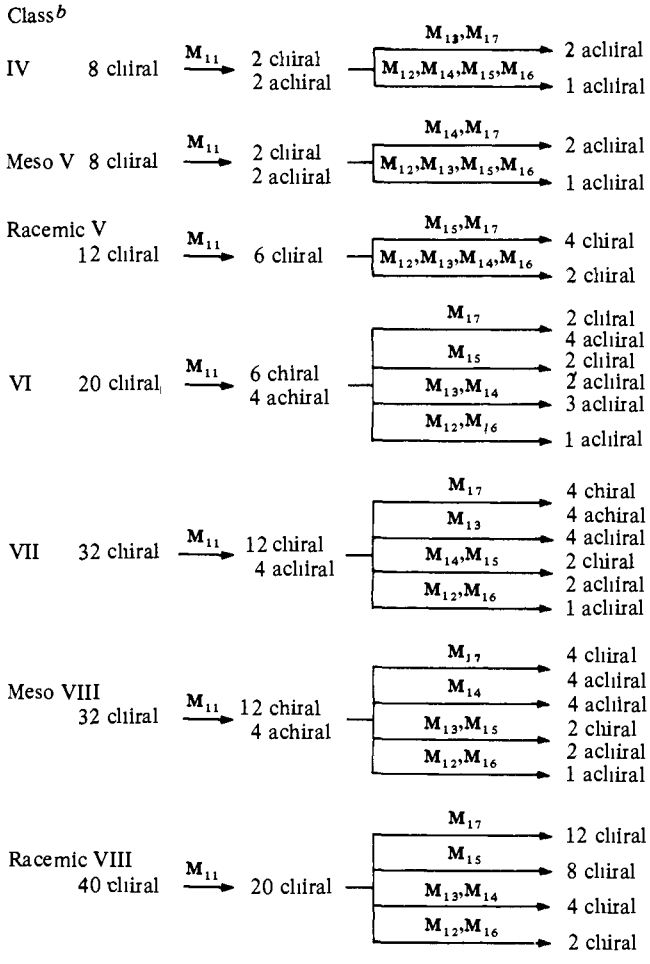

[a] Number and kind of residual stereoisomers under the action of various rearrangement modes (see text). [b] See Table VII.

Scheme II[a]

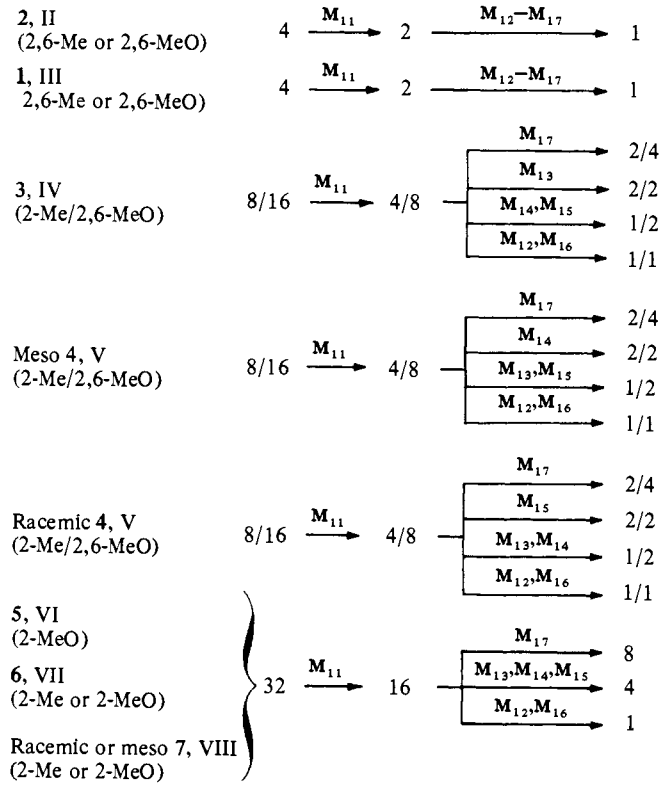

[a] Number of NMR signals under the action of various rearrangement modes, in an achiral medium, and in the absence of accidental isochrony. [b] Boldfaced numeral refers to compound number and roman numeral to class (Table VII). Symbols in parentheses represent the signal generating groups and refer to the numbers of signals in the scheme.

Between the two approaches illustrated in Schemes I and II, we feel that the advantages of DNMR analysis far outweigh the potentially arduous procedure of separating residual stereoisomers. Not all of the five classes (IV-VIII) need be investigated. For example, the DNMR effects of **5**, **6**, and **7** are identical. In principle, a single one of the examples in classes IV-VIII could distinguish the three-ring flip ($\mathbf{M}_{12}$) from a two-ring flip ($\mathbf{M}_{13}$, $\mathbf{M}_{14}$, or $\mathbf{M}_{15}$), while any two of **3**, racemic **4**, and meso **4** could distinguish among the various two-ring flips.

It should be noted that substitution pattern a_2CHCHb_2 (classes II, IV, and VII) will yield the same number of signals as for *ab*CHCH*ab* (classes III, V, and VIII, respectively), except that the effects of $\mathbf{M}_{13}$ and $\mathbf{M}_{14}$ for meso *ab*CHCH*ab* ($\mathbf{M}_{13}$ and $\mathbf{M}_{15}$ for racemic *ab*CHCH*ab*) will be switched. This switching can be intuitively justified if we consider the skeletal symmetry (**S**) and the "mode symmetry" (**T**), i.e., the symmetry of the idealized two-ring flip transition state associated with that mode. **S** for a_2CHCHb_2 and **T** for $\mathbf{M}_{13}$ are $\mathbf{C}_s$; **S** for meso *ab*CHCH*ab* and **T** for $\mathbf{M}_{14}$ are $\mathbf{C}_i$; and **S** for racemic *ab*CHCH*ab* and **T** for $\mathbf{M}_{15}$ are $\mathbf{C}_2$. If **S** and **T** are the same, constitutionally identical rings are both flipped or both nonflipped. On the other hand, if **S** and **T** are not the same, one of each type of ring is flipped, while the other is nonflipped.

Experimental Section

DNMR Measurements. ^{1}H NMR spectra were recorded on a Varian A-60D spectrometer equipped with variable-temperature accessories. Temperature measurements were based on the chemical-shift separation of the protons of a methanol or an ethylene glycol sample, and utilized the temperature-shift correlation of Van Geet.[32] Temperatures are considered to be accurate to ±2°, although within a given series of measurements smaller differences (ca.±0.5°) were considered significant. Saturation of the NMR signals was avoided. Unless otherwise specified, NMR samples were ca. 25% v/v solutions with ca. 5% v/v Me_4Si. The line-shape analyses[22] were performed on a CDC-6600 computer.

The ^{1}H NMR spectrum of TME in hexachloro-1,3-butadiene at 40 °C features resonances at δ 1.68 (peak 1), 1.81 (2), 1.90 (3), 1.99 (4), 2.04 (5), and 2.08 (6).

The ^{1}H NMR spectrum of racemic **1** in $CDCl_3$ at −4° features resonances for the six methoxy groups at δ 3.02 (peak 1), 3.26 (2), 3.46 (3), 3.50 (4), 3.61 (5), and 3.63 (6). For assignments, see text and part I.

The chemical shifts of resonances 1-6 are temperature dependent and shifts in the region of coalescence were estimated by linear extrapolation from the region where direct measurements were possible. The temperature dependence was expressed in terms of the difference in chemical shift, in hertz, of a given signal i and reference signal 2 as a function of temperature (T, °C). Straight lines with good correlation coefficients ($\rho > 0.99$) were obtained on plotting $\Delta\nu_i$ against T. An exchange matrix for use in the Saunders computer program[22] was constructed in which signals 1 and 3, 2 and 4, and 5 and 6, were allowed to exchange. The ratio of rates of the two processes involved (i.e., $A\bar{A} \rightarrow B\bar{B}$ and $B\bar{B} \rightarrow A\bar{A}$) was taken equal to 1.37:1. The calculated rate constants at five temperatures were used to calculate $\Delta H^{\ddagger}$ and $\Delta S^{\ddagger}$ from a least-squares treatment of ln (k/T) vs. $(1/T)$[33] (ρ = 0.999) for the diastereomerization process and the resulting parameters were employed to derive $\Delta G^{\ddagger}_{40}$ for this process as reported in the text. The value of $\Delta S^{\ddagger}$ calculated for racemic **1** was small, but since the values obtained for $\Delta H^{\ddagger}$ and $\Delta S^{\ddagger}$ from line-shape methods are sometimes questionable,[34] they are not reported here.

The ^{1}H NMR spectrum of *meso*-**1** in $CDCl_3$ at −1° features six signals in the methoxy region: δ 3.09 (peak 1), 3.25 (2), 3.47 (3), 3.57 (4), 3.70 (5), and 3.73 (6) ppm. For assignments, see text and part I.

In this case also the chemical shifts of resonances 1-6 show a slight variation with temperature. The line-shape analysis[22] of this spectrum and those obtained at higher temperatures was carried out as described above for racemic **1**, with the exception that signals 1 and 3, 2 and 4, and 5 and 6, were allowed to exchange at the same rate. The calculated rate constants at eight temperatures were used to calculate $\Delta H^{\ddagger}$ and $\Delta S^{\ddagger}$, as described above, and the resulting parameters were employed to derive $\Delta G^{\ddagger}_{50}$ for the enantiomerization process, as reported in the text. The value of $\Delta S^{\ddagger}$ calculated for *meso*-**1** was small.

Acknowledgment. We gratefully acknowledge support of this research by the North Atlantic Treaty Organization (Research Grant No. 902) and the National Science Foundation (MPS74-18161).

References and Notes

(1) (a) University of Catania; (b) Princeton University.
(2) P. Finocchiaro, D. Gust, W. D. Hounshell, J. P. Hummel, P. Maravigna, and K. Mislow, *J. Am. Chem. Soc.*, preceding paper in this issue.
(3) J. I. Musher, *J. Am. Chem. Soc.*, **94**, 5662 (1972).
(4) P. Finocchiaro, D. Gust, and K. Mislow, *J. Am. Chem. Soc.*, **96**, 3198, 3205 (1974).
(5) (a) M. G. Hutchings, J. G. Nourse, and K. Mislow, *Tetrahedron*, **30**, 1535 (1974); (b) J. G. Nourse and K. Mislow, *J. Am. Chem. Soc.*, **97**, 4571 (1975).
(6) K. Mislow, *Acc. Chem. Res.*, **9**, 26 (1976).
(7) W. Hässelbarth and E. Ruch, *Theor. Chim. Acta*, **29**, 259 (1973).
(8) D. Gust and K. Mislow, *J. Am. Chem. Soc.*, **95**, 1535 (1973).
(9) W. G. Klemperer, *J. Chem. Phys.*, **56**, 5478 (1972).
(10) D. Gust, P. Finocchiaro, and K. Mislow, *Proc. Natl. Acad. Sci. U.S.A.*, **70**, 3445 (1973).
(11) H. C. Longuet-Higgins, *Mol. Phys.*, **6**, 445 (1963).
(12) The number of double cosets (n) can be found using the formula:[7]

$$n = \frac{|\mathbf{G}_{64}|}{|\mathbf{C}_2|^2} \sum_{r=1}^{k} \frac{|\mathbf{C}_r \cap \mathbf{C}_2|^2}{|\mathbf{C}_r|}$$

where $\mathbf{C}_r$ is one of the k conjugacy classes in $\mathbf{G}_{64}$.
(13) These 17 modes correspond to those for tetraarylmethanes[5b] as follows: 1 → 13; 2 and 3 → 15; 4 and 5 → 16; 6 and 7 → 17; 8 and 9 → 18; 10 → 19; 11 → 21; 12a,b → 23; 13 and 14 → 24; 15a,b → 20; 16a,b → 22; 17 → 14.
(14) For tetraarylethylenes, which are stereochemically correspondent to tetraarylethanes,[2] there are 14 double cosets (all self-inverse) of the point group $\mathbf{D}_2$, in the feasible permutation-inversion group, $\mathbf{G}_{128}$ (defined in footnote 21 of ref 2), which correspond to these 17 modes when $\mathbf{M}_2 + \mathbf{M}_3$, $\mathbf{M}_6 + \mathbf{M}_7$, and $\mathbf{M}_8 + \mathbf{M}_9$ are combined. Thus, an analysis of such systems would be analogous to the one presented in the present paper for tetraarylethanes.

(15) J. P. Hummel, D. Gust, and K. Mislow, *J. Am. Chem. Soc.*, **96**, 3679 (1974).
(16) (a) J. D. Andose and K. Mislow, *J. Am. Chem. Soc.*, **96**, 2168 (1974); (b) M. R. Kates, J. D. Andose, P. Finocchiaro, D. Gust, and K. Mislow, *Ibid.*, **97**, 1772 (1975).
(17) These are an extension of the flip mechanisms originally postulated for triarylcarbenium ions by R. J. Kurland, I. I. Schuster, and A. K. Colter, *J. Am. Chem. Soc.*, **87**, 2279 (1965).
(18) J. Brocas, R. Willem, D. Fastenakel, and J. Buschen, *Bull. Soc. Chim. Belg.*, **84**, 483 (1975).
(19) H. S. Gutowsky and C. H. Holm, *J. Chem. Phys.*, **25**, 1228 (1956).
(20) H. Lankamp, W. Th. Nauta, and C. MacLean, *Tetrahedron Lett.*, 249 (1968).
(21) A clear-cut choice could be made by introducing a prochiral group[15] or by operating in a chiral environment.
(22) The computer program used was adapted from one developed by M. Saunders (see M. Saunders in "Magnetic Resonances in Biological Systems", A. Ehrenberg, B. C. Malmström, and T. Vänngard, Ed., Pergamon Press, New York, N.Y., 1967, p 85). We are grateful to Professor Saunders for providing us with a copy of the program, and to Drs. J. D. Andose and V. Librando for the modifications.
(23) H. Shanan-Atidi and K. H. Bar-Eli, *J. Phys. Chem.*, **74**, 961 (1970).
(24) Within the limitations of the present evidence, steric arguments must be resorted to in order to differentiate between modes $\mathbf{M}_{11}$ and $\mathbf{M}_{17}$ as threshold mechanisms. The group generated by these two modes ($\mathbf{G}_{4a}$ and $\mathbf{G}_{4b}$, respectively; see Table VI) contains elements in the same conjugacy classes of $\mathbf{G}_{64}$ and thus the same number of isomers and NMR signals will always be expected under the action of each of these two modes. Since there is only one mode equivalent flip mechanism for each, there is no possibility of differentiating between them on the basis of diastereomeric mode equivalent pathways.
(25) The first example of residual diastereotopism in a molecular propeller was reported by J. C. Martin and co-workers,[26] who found that the *o*-methyl and *o*-methoxy signals in dimesityl(2,4,6-trimethoxyphenyl)methane coalesce at −20 and 145 °C, respectively. The residual diastereotopism of the *o*-methoxy groups at temperatures above −20° and below 145° may be viewed[4,8] as the ghost of the residual stereoisomerism in dimesityl(3-methyl-2,4,6-trimethoxyphenyl)methane, an as yet unreported compound which will predictably[8] exist in two diastereomeric forms.
(26) M. J. Sabacky, S. M. Johnson, J. C. Martin, and I. C. Paul, *J. Am. Chem. Soc.*, **91**, 7542 (1969).
(27) D. Hellwinkel, M. Melan, W. Egan, and C. R. Degel, *Chem. Ber.*, **108**, 2219 (1975).
(28) J. F. Blount and K. Mislow, *Tetrahedron Lett.*, 909 (1975).
(29) P. Finocchiaro, D. Gust, and K. Mislow, *J. Am. Chem. Soc.*, **96**, 2176 (1974).
(30) M. G. Hutchings, J. d. Andose, and K. Mislow, *J. Am. Chem. Soc.*, **97**, 4562 (1975).
(31) See footnote 21 of part I.
(32) A. L. Van Geet, *Anal. Chem.*, **42**, 679 (1970); **40**, 2227 (1968).
(33) The transmission coefficient was assumed to be unity.[34]
(34) See G. Binsch, *Top. Stereochem.*, **3**, 97 (1968).

Reactions of the K-Region Oxides of Carcinogenic and Related Polycyclic Hydrocarbons with Nucleophiles: Stereochemistry and Regioselectivity

Frederick A. Beland and Ronald G. Harvey*

Contribution from the Ben May Laboratory, University of Chicago, Chicago, Illinois 60637. *Received January 9, 1976*

Abstract: Reactions of the "K-region" oxides of a series of carcinogenic and related polycyclic hydrocarbons with the model nucleophile *tert*-butyl mercaptide afford the products of trans-stereospecific addition to the oxide ring in aqueous dioxane or addition-dehydration to *tert*-butylthioarenes in THF. Product structures accord with regioselective attack at the most electrophilic center(s) in agreement with MO theoretical prediction. Addition to the K-region oxide of the potent carcinogen 7,12-dimethylbenz[*a*]anthracene takes place selectively at the 6 position with rearrangement during dehydration to furnish 7,12-dimethyl-5-*tert*-butylthiobenz[*a*]anthracene. Structural assignments are aided by 270-MHz high-resolution NMR spectroscopy utilizing benzylic coupling constants, lanthanide-induced shifts, and nuclear Overhauser enhancement measurements in the 1:1 adducts and an observed strong downfield shift of the aryl protons adjacent to the thio ether group in the alkylthioarenes.

The hypothesis by Miller and Miller[1] that carcinogens or their metabolically activated derivatives act as electrophiles which initiate tumor formation through covalent interaction with nucleic acids or proteins is supported by an expanding body of evidence.[2] In the case of the carcinogenic hydrocarbons, the nature of the active intermediate is not established. However, the K-region oxides[3] have been shown to bind covalently to nucleic acids and proteins in vivo,[4-6] to be more active than the parent hydrocarbons in the transformation of cells in culture[7] and more highly mutagenic than either the hydrocarbons[8] or the non-K-region oxides.[9] On the other hand, diol oxide derivatives of benzo[*a*]pyrene (BaP) and benz[*a*]anthracene (BA) recently have been suggested[10,11] to be the principal metabolites of these hydrocarbons bound to DNA in vivo.

The structures of the hydrocarbon nucleic acid and protein conjugates have not been established. Hydrolysis of the nucleic acid conjugates of the K-oxides of BaP and 7,12-dimethylbenz[*a*]anthracene (DMBA) gave products in which the hydrocarbon was bound principally to guanosine.[5,6,12] Recent experiments have revealed these products to be further separable by HPLC into several, presumably isomeric, components.[13] Because of the low extent of binding, the quantities of these bound adducts isolable are quite small, i.e., submilligram, adding to the difficulty of ultimate structural elucidation.

In order to gain some insight into the nature of these reactions, particularly their regio- and stereoselectivity, and to obtain NMR and other data on compounds of authentic structure, we undertook to investigate the reactions of a series of K-region oxides, including several derivatives of carcinogenic hydrocarbons, with the model nucleophile *tert*-butyl mercaptide anion. The choice of this reagent was dictated by the known effectiveness of sulfur nucleophiles in the cleavage of epoxide rings[16] and the anticipated relative simplicity of the NMR spectra. In addition, *tert*-butyl mercaptan provides a convenient model for cysteine and glutathione, the former the principal site of reaction of arene oxides on proteins,[14] the latter one of the principal means of detoxification of arene oxides in vivo.

No systematic study of the reactions of the K-region arene oxides of carcinogenic hydrocarbons with nucleophiles has been reported. Swaisland et al.[15] investigated the relative reactivity of various K-region oxides with 4-(*p*-nitrobenzyl)pyridine, but did not determine product structure. Reactions of the benzene and naphthalene (non-K-region) oxides with several nucleo-